https://doi.org/10.5194/amt-2019-489
Preprint. Discussion started: 9 March 2020

Atmospheric Measurement Techniques Discussions

Development of an Automatic Linear Calibration Method for High Resolution Single Particle Mass Spectrometry: Improved Chemical Species Identification for Atmospheric Aerosols

Authors: Shengqiang Zhu[1], Lei Li[2], Shurong Wang[1], Mei Li[2], Yaxi Liu[1], Xiaohui Lu[1], Hong Chen[1], Lin Wang[1, 3], Jianmin Chen[1, 3], Zhou Zhen[2], Xin Yang*[1, 3] and Xiaofei Wang*[1, 3]

[1]*Shanghai Key Laboratory of Atmospheric Particle Pollution and Prevention, Department of Environmental Science and Engineering, Fudan University, Shanghai 200433, China*

[2]*Institute of Mass Spectrometer and Atmospheric Environment, Jinan University, Guangzhou, 510632, China*

[3]*Shanghai Institute of Pollution Control and Ecological Security, Shanghai 200092, China*

Atmospheric Measurement Techniques Discussions

March 8th, 2020

*To whom correspondence should be addressed.

Correspondence to:
Xiaofei Wang
Email: xiaofeiwang@fudan.edu.cn Tel: +86-21-31242526
Xin Yang
Email: yangxin@fudan.edu.cn Tel: +86-21-31245272

https://doi.org/10.5194/amt-2019-489
Preprint. Discussion started: 9 March 2020

Atmospheric Measurement Techniques Discussions

Abstract

The mass resolution of laser desorption ionization (LDI) single particle aerosol mass spectrometry (SPAMS) is usually low (~500), which has been greatly improved by recent development of delayed ion extraction technique. However, due to large fluctuations among LDI processes during each laser shot, accurate calibration of mass-to-charge ratio for high resolution SPAMS spectra is challenging. Here we developed an automatic linear calibration method to improve the accuracy of mass-to-charge (m/z) measurement for single atmospheric aerosol particles. Laboratory generated sea spray aerosol and atmospheric ambient aerosol were tested. After the calibration, the fluctuation ranges of the reference ions (e.g. Pb^+ and SO_4^+) m/z reaches ±0.018 for sea spray aerosol and ± 0.024 for ambient aerosol in average mass spectra. With such m/z accuracy, the HR-SPAMS spectra of sea spray aerosol can easily identify elemental compositions of organic peaks, such as C_x, C_xH_y and $C_xH_yO_z$. While the chemical compositions of ambient aerosols are more complicated, C_xH_y, $C_xH_yO_z$ and CNO peaks can also be identified based on their accurate mass. With the improved resolution, the time series of peaks with small m/z differences can be separated and measured. In addition, it is also found that applying high resolution data with enhanced mass calibration can significantly affect particle classification (identification) using the ART-2a algorism, which classify particles based on similarities among single particle mass spectra.

https://doi.org/10.5194/amt-2019-489
Preprint. Discussion started: 9 March 2020


Atmospheric Measurement Techniques Discussions

1. Introduction

Atmospheric aerosols significantly impact radiative forcing, cloud formation and human health(Ackerman et al., 2004; Zhang and Kin-Fai, 2012). They originate from various sources and undergo many atmospheric aging processes, resulting in an extremely complicated mixture of particles with a large range of sizes and chemical compositions. The mixture is usually referred as "mixing state". Measurement of aerosol mixing state requires single particle characterization techniques. Utilizing laser ablation/ionization of singe aerosol particle, Single Particle Aerosol Mass Spectrometer (SPAMS) has been widely used to measure chemical compositions and sizes of aerosols in real-time(Moffet and Prather, 2009; Murphy, 2010; Sullivan and Prather, 2005). Based on this technique, ART-2a and other algorithms had been developed to classify the ambient particles based on their mass spectra and identify their sources and aging paths (Reinard et al., 2007; Zelenyuk and Imre, 2009).

However, SPAMS with LDI has several serious limitations(Manuel et al., 2006; Wenzel et al., 2003). A major issue is that the mass resolution of the SPAMS is relatively low (~500) and the accuracy of m/z (mass to charge ratio) is usually at integer level, resulting in uncertainties about the identification of chemical species (Nash et al., 2006; Pratt and Prather, 2012; Qin et al., 2006). Due to the low mass resolution, many organic and inorganic peaks cannot be separated, such as K^+ /$C_3H_3^+$ with the integer m/z at 39, Al^+ /$C_2H_3^+$ with the integer m/z at 27 and CN^- /$C_2H_2^-$ with the integer m/z at -26 (Li et al., 2018). To identify these chemical species, A SPAMS with higher mass resolution and better m/z accuracy is needed.

Recently, Li et al., significantly increased SPAMS's mass resolution to ~2000 by applying delayed ion extraction technique, which combined a standard rectangular extraction pulse with an exponential pulse (Li et al., 2018). This updated SPAMS is called high resolution (HR)-SPAMS. Unfortunately, in spite of resolution enhancement with this new technique, ion peak position was still very sensitive to initial ion coordinate and speed (Chudinov et al., 2019), i.e. the calibration parameter for each mass spectrum is significantly different.

https://doi.org/10.5194/amt-2019-489
Preprint. Discussion started: 9 March 2020


Atmospheric Measurement Techniques Discussions

Therefore, in order to get accurate m/z, Chudinov et al. used several peaks with known m/z to calibrate every SPAMS spectrum for $Pb(NO_3)_2$ and NaI particles produced from an atomizer.

However, atmospheric particles are extremely complicated with a wide range of chemical compositions and sizes (Zhang et al., 2013), which bring much greater challenge to properly calibrating each SPAMS mass spectra and obtaining accurate m/z measurement. We need to develop a new MS calibration method for atmospheric aerosols and evaluate its performance comprehensively.

In this study, we report a calibration method for single particle high resolution mass spectra data. Its performance had been evaluated in detail for both laboratory-generated sea spray aerosol and ambient aerosol. In addition, the impact of using high resolution SPAMS data on particle classification by ART-2a algorithm was accessed.

2. Experimental Section

2.1 High Resolution Single Particle Aerosol Mass Spectrometer (HR-SPAMS)

The detailed description of HR-SPAMS (Hexin Analytical Instrument Co., Ltd., China) can be found elsewhere(Li et al., 2018). Briefly, a HR-SPAMS consists of an aerodynamic lens as its particle inlet, two laser beams system for particle sizing, a UV laser for LDI and a bipolar time-of-flight mass analyzer for the detection of positive and negative ions. Positive and negative ions are detected by two z-shape bipolar TOF reflectron mass analyzers. The size detection range of HR-SPAMS is 200-2000 nm. As introduced before, this HR-SPAMS used delayed ion extraction technique.

2.2 Laboratory generated sea spray aerosol

Sea spray aerosol was produced by water jet method. In a sea spray aerosol production tank, a seawater jet was hitting seawater surface and producing bubbles, which would rise to the surface and burst. Bubble bursting process produces sea spray aerosols. Seawater was collected at Fengxian, Shanghai (30°92'N and 121°47'E) on March 30th 2019 (Fig.S1).

https://doi.org/10.5194/amt-2019-489
Preprint. Discussion started: 9 March 2020


Atmospheric Measurement Techniques Discussions

2.3 Ambient aerosol sampling

Ambient aerosol sampling was conducted at Fudan university, Shanghai (31°20'N and 121°30'E) on May 29th 2019 (Fig.S1). The ambient particles were dried a diffusional dryer before being sampled by the HR-SPAMS.

3. Development of Calibration Methods

3.1 Automatic linear calibration method

To improve the accuracy of m/z for HR-SPAMS spectra, an automatic linear calibration method has been developed. Noticeably, due to the technical limitation of data acquisition, the whole HR-SPAMS spectrum is not continuous but divided by a large number of m/z bins, which are described in Fig.S2. Here we denote "m/z bin value" as the median m/z value of each bin.

The linear calibration method is described as the following steps:

Step 0: The SPAMS data was coarsely-calibrated by the traditional method, which usually selected a few particles with distinct ion patterns, i.e. the molecular composition of some distinct peaks in the mass spectra can be easily identified. Then, the time of flight of these peaks and the m/z of the corresponding ions were used to calculate a set of calibration parameters for both positive and negative spectra. The parameters were then applied to the whole mass spectra dataset, and the coarsely-calibrated was completed.

Step 1: a pool of ion peaks in the single particle mass spectra were selected as the potential m/z calibration reference ions. The selection criteria are (1) these peaks should be present in most of the spectra; (2) the identification of these ion peaks should not be significantly affected by other adjacent peaks. For example, $27[Al]^+$ was not selected, as its adjacent peak $27[C_2H_3]^+$ may affect the peak shape and identification of $27[Al]^+$.

According to the previous research, possible peak assignments for the m/z of reference ions for sea spray aerosol and ambient aerosol were listed on Table 1(Bertram et al., 2018; Collins et al., 2014; Tsunogai et al., 1972; Wang et al., 2016; Wang et al., 2019). For sea

https://doi.org/10.5194/amt-2019-489
Preprint. Discussion started: 9 March 2020


Atmospheric Measurement Techniques Discussions

spray aerosol, according to several studies (Bertram et al., 2018; Collins et al., 2014; Tsunogai et al., 1972), the reference ions with m/z 23 24 39 -35 -37 were 23[Na]$^+$ 24[Mg]$^+$ 39[K]$^+$ -35[Cl]$^-$ and -37[Cl]$^-$ respectively. And Collins et al. shows that the reference ions with m/z 81, 83, -26, -42, -58, -129, and -131 were 81[Na_2Cl]$^+$, 83[Na_2Cl]$^+$, -26[CN]$^-$, -42[CNO]$^-$, -58[NaCl]$^-$, -129[$MgCl_3$]$^-$, and -131[$MgCl_3$]$^-$, respectively(Collins et al., 2014). Due to the fact that Na, Mg and K were abundant in sea spray aerosol, the reference ions with m/z 113 and 115 should be 113[K_2Cl]$^+$ and 115[K_2Cl]$^+$.Thus, in this study, we select 23[Na]$^+$, 24[Mg]$^+$, 39[K]$^+$, 81[Na_2Cl]$^+$, 83[Na_2Cl]$^+$, 113[K_2Cl]$^+$, 115[K_2Cl]$^+$, -35[Cl]$^-$, -37[Cl]$^-$, -26[CN]$^-$, -42[CNO]$^-$, -129[$MgCl_3$]$^-$, -131[$MgCl_3$]$^-$, -58[NaCl]$^-$ as the potential reference ions for sea spray aerosols.

For the ambient aerosol, according to the previous ambient SPAMS measurements(Wang et al., 2016; Wang et al., 2019), the reference ions with m/z 12, 23, 36, 39, 56, 207, 208, and 209 were assigned to 12[C]$^+$, 23[Na]$^+$, 36[C_3]$^+$, 39[K]$^+$, 56[Fe]$^+$, 207[Pb]$^+$, 208[Pb]$^+$ and 209[Pb]$^+$, the reference ions with m/z -26, -35, -46, -62, -96, and -97 were assigned to -26[CN]$^-$, -35[Cl]$^-$, -46[CNO]$^-$, -62[NO_2]$^-$, -96[SO_4]$^-$ and -97[HSO_4]$^-$, respectively. Therefore, in this study, we select the 12[C]+, 23[Na]$^+$, 39[K]$^+$, 36[C_3]$^+$, 56[Fe]$^+$, 208[Pb]$^+$, 206[Pb]$^+$, 207[Pb]$^+$, -62[NO_3]$^-$, -26[CN]$^-$, -35[Cl]$^-$, -96[SO_4]$^-$, -46[NO_2]$^-$, -97[HSO_4]$^-$ as the potential reference ions for ambient aerosols.

Step 2: a set of reference ions was chosen from the potential reference ion pool for each spectrum. The selection was based on the absolute ion intensity of the reference ions in this spectrum. They must be greater than a threshold, e.g. we set 15 a.u. for ambient aerosol and 8 a.u. for sea spray aerosol, respectively. A particle was discarded from the spectra database if it did not have enough reference ions (the minimum number of reference ions was set to be 5) in either positive or negative mass spectrum.

Step 3: the reference ions were used to calibrate m/z for mass spectra of each particle. As introduced before, a HR-SPAMS spectrum consists of a number of bins. The measured m/z bin values of the reference ions were calibrated based on their theoretic (or true) m/z bin values. A linear regression between the two set of variables (measured vs. theoretic m/z bin

https://doi.org/10.5194/amt-2019-489
Preprint. Discussion started: 9 March 2020


Atmospheric Measurement Techniques Discussions

values) was conducted, and two calibration parameters (a slope and an intersect) were obtained. After applied calibration parameters, the m/z of the whole spectrum had been corrected. However, the corrected m/z may not be equal to the m/z bin value. Thus, we assigned a m/z bin value to each corrected m/z based on proximity principle. Finally, mass spectra with well calibrated bin value can be obtained for each single particle.

A GUI program for this automatic linear calibration method had been developed for the sake of easy use (Fig. 1). The MATLAB codes for this GUI and the automatic linear calibration method are open access and available at https://github.com/zhuxiaoqiang-fdu/zhuxiaoqiang-fdu.

3.2 Evaluation of the calibration method

In this study, a total of 5,130 sea spray aerosol particles and 5,007 ambient aerosol particles were analyzed. And 4,624 sea spray particles and 1,409 ambient particles were successfully calibrated. Figure 2 shows that the calibration curves for a random selected sea spray aerosol particle and ambient aerosol particle. The adj-R^2 coefficients of both calibration curves are equal to ~1, demonstrating that this calibration method is effective and accurate. All the slopes and intercepts of the linear calibration can be found in the Fig.S3 and Fig.S4. In addition, Figure 3a and 3b report a comparison of m/z distributions of reference ions between before and after automatic linear calibration. The results show that the fluctuations of the reference ions m/z were significantly reduced after automatic linear calibration. The average m/z deviation of the reference ions was reduced from ~0.04 to ~0.001 for sea spray aerosol, and from ~0.035 to ~0.006 for ambient aerosol, respectively.

3.3 Automatic linear calibration method with a larger reference ion pool

It is important to note that a large number of ambient particles were filtered because their spectra did not have 5 or more reference peaks to conduct calibrations. Especially, only ~29.0% of total ambient particles had sufficient number of reference ions in their positive spectra. To solve this problem, extra reference ions, including 67$[VO]^+$, 67$[C_5H_7]^+$, 89$[C_7H_5]^+$, 89$[Na_2BO_2]^+$, 102$[C_8H_6]^+$, 102$[CaNO_3]^+$, were added into the original positive reference ion pool. Obviously, these ions share the same integer m/z value with other ions.

https://doi.org/10.5194/amt-2019-489
Preprint. Discussion started: 9 March 2020


Atmospheric Measurement Techniques Discussions

We needed to identify them using additional information other than their integer m/z values.

The specific reference ions were determined by their coarsely-calibrated m/z. Table S2 shows that the m/z deviation ranges of the reference positive ambient ions in coarsely-calibrated spectra before automatic linear calibration were around 0.011~0.048, while the m/z differences between 67$[VO]^+$ and 67$[C_5H_7]^+$, 89$[C_7H_5]^+$ and 89$[Na_2BO_2]^+$, 102$[C_8H_6]^+$ and 102$[CaNO_3]^+$ were 0.1213, 0.0622, and 0.083, respectively, which were larger than the m/z deviations of these reference ions in coarsely-calibrated spectra. Therefore, the coarsely-calibrated spectra can be used to determine these specific reference ions. With these additional potential reference ions, a total of 2490 ambient particles were calibrated, much more than the previous analysis (1,409 ambient particles). The deviations from theoretical m/z for applying this expanded ion pool are summarized in Table S3. The average m/z deviation of the reference ions is ~0.0068.

4. Application to atmospheric aerosols measurement

4.1 HR-SPAMS measurement of sea spray aerosol

SPAMS data usually contains a large number of individual mass spectra. It is impossible to manually analyze every spectrum from a large dataset. Averaging a number of mass spectra is often preferred. However, to obtain averaged high-resolution spectrum, each spectrum must be well calibrated. Therefore, it would be very interesting to see what new information can be obtained from HR-SPAMS measurement of aerosols with the automatic calibration method. Figure 4 reports the average positive and negative mass spectra for the laboratory generated sea spray aerosols. Similar to the low-resolution sea spray aerosol mass spectra, they contain major peaks of Na^+, Mg^{2+}, K^+, Na_2Cl^+, CN^-, Cl^-, CNO^-, $NaCl^-$, $NaCl_2^-$ and $MgCl_3^-$, as well as many smaller peaks, such as Ca^+, SiO_2^-/SiO_3^-, and KCl_2^-. With the improved m/z measurement, many peaks, which cannot be determined by integer resolution mass spectra, now can be clearly identified (Table 2). For example, the ion with m/z at 27.0267 is $C_2H_3^+$ rather than Al^+. The ion with m/z at 76.9336 is $CaCl^+$ rather than $C_6H_5^+$. And some sulfur containing organic ions, such as CS^+, can be determined. Surprisingly, we can identify the presence of HCO_2^- and $CaCO_3^-$, demonstrating that carbon hydrates were contained in sea spray aerosols.

https://doi.org/10.5194/amt-2019-489
Preprint. Discussion started: 9 March 2020


Atmospheric Measurement Techniques Discussions

241

242 **4.2 HR-SPAMS measurement of atmospheric aerosol**

243 Laboratory generated sea spray aerosol can be viewed as a relatively simple aerosol system,
244 while the chemical compositions of ambient aerosols are much more complicated. Figure
245 5 shows the averaged HR-SPAMS mass spectra of the ambient aerosols sampled at Fudan
246 University Jiangwan Campus on May 29th, 2019. With the improved m/z measurement,
247 many organic ions, such as C_x, C_xH_y, and $C_xH_yO_z$ can be directly identified (Table 3). Also,
248 we can separate the organic and inorganic species more directly with the high mass
249 resolution. For instance, $C_6H_8^+$ can be clearly distinguished from possible interference of
250 Ca_2^-, TiO_2^+ and $NaKO^+$. $C_{10}H^-$ can also be identified from possible assignment of $NaSO_4^-$
251 etc.

252

253 **4.3 Time variation of HR-SPAMS measurement**

254 With the high mass resolution of HR-SPAMS and enhanced m/z calibration, we were able
255 to obtain an average mass spectrum from many particles. The accurate m/z values in the
256 average mass spectrum can be used to separate peaks with close m/z and track their
257 intensity variations. Here we conducted a time variation measurement for ambient aerosol
258 from 11:00 on May 29th to 11:00 on May 30th 2019. We selected first 500 particles collected
259 by SPAMS during every hour for elemental analysis. Figure 6 shows that the peak at m/z
260 41 has a bimodal structure, whose m/z were at 40.9546±0.0105 and 41.0194±0.0105,
261 respectively. Thus the peak with the smaller m/z is an isotope of K^+(theoretical m/z value
262 of $^{41}K^+$ = 40.96182, theoretical m/z bin value of $^{41}K^+$ = 40.9667; this peak also follows the
263 isotopic pattern of K) and the other peak should be $C_3H_5^+$(theoretical m/z value 41.03913,
264 theoretical m/z bin value 41.03). Figure 6 shows that HR-SPAMS was able to separately
265 measure the time series of these two peaks with a small m/z difference. In contrast, it is
266 impossible for a LR-SPAMS to provide such detailed time variation measurement of these
267 peaks.

268

269 **4.4 Particle classification by ART-2a**

270 Adaptive resonance theory neural network (ART-2a) is a widely-used method to classify
271 particles based on the similarity among their mass spectra (Song et al., 1999). Here we

https://doi.org/10.5194/amt-2019-489
Preprint. Discussion started: 9 March 2020


Atmospheric Measurement Techniques Discussions

make a comparison of ART-2a classification between the HR-SPAMS data and traditional low resolution (LR)-SPAMS data. Particles with the positive and negative spectra were analyzed by ART-2a with a learning rate of 0.05, a vigilance factor of 0.7, and an iteration number of 20. The previous ambient aerosol SPAMS dataset was used. The LR-SPAMS data, whose m/z was at integer level, was generated by summing high resolution SPAMS peaks in each integer m/z bin. The classification results show that the HR-SPAMS data was grouped to 93 categories and the top 45 categories accounted for 96 percent of all particles. The particle number of the first eight categories was 122, 101, 99, 86, 82, 70, 68 and 60 respectively. In contrast, the LR-SPAMS data was only grouped to 33 categories in total and the top 20 categories accounted for the 96 percent of all particles. The particle number of the first eight categories was 170, 118, 107, 107, 106, 92, 90 and 88 respectively. The detailed results can be found in the Fig.S5-S6. Obviously, ART-2a classification of high resolution SPAMS data generated more particle categories. This is mainly because HR-SPAMS mass spectra can differentiate peaks with close m/z, which may be viewed as one peak in LR-SPAMS data.

The ART-2a classification of the HR-SPAMS results (Fig.S6) show that the signal at 23[Na^+] in the second particle type was stronger than first particle type while the signals at 26[CN^-] and 42[CNO^-] were weaker in first particle type. In contrast, these two first particle types were lumped together into the first particle type in the LR-SPAMS classification results (Fig.S5). The third, fourth and fifth particle types from the HR-SPAMS classification results contain strong signals at 26[CN^-], 42[CNO^-], 46[NO_2^-], 62[NO_3^-] and 97[HSO_4^-], while these three particle types were lumped together as the second particle type in the LR-SPAMS classification results. In general, ART-2a classification of HR-SPAMS would generate more particle types than that of LR-SPAMS. Given HR-SPAMS spectra have much more detailed chemical information about particles, we would propose that the ART-2a classification of HR-SPAMS might be more accurate.

5. Conclusion

An automatic linear calibration method had been developed for data analysis of high-resolution SPAMS data. This technique can significantly improve the m/z accuracy of

https://doi.org/10.5194/amt-2019-489
Preprint. Discussion started: 9 March 2020


Atmospheric Measurement Techniques Discussions

SPAMS spectra for atmospheric aerosol samples. The analysis of HR-SPAMS data for laboratory generated sea spray aerosols shows many details of its chemical compositions. For example, many organic ions, such as $C_2H_3^+$ and CS^+, can be directly determined. The chemical compositions of ambient aerosols are much more complicated. It is found that, besides major ions (e.g. Na^+, K^+, Ca^+, Fe^+, Cl^-, CN^-, NO_3^- and HSO_4^-), C_xH_y, $C_xH_yO_z$ and CNO^- can be identified. With this method, HR-SPAMS can also separately measure the time series of peaks, whose m/z are close to each other (e.g. $^{41}K^+$ with the theoretical m/z value at 40.96182 and $C_3H_5^+$ with the theoretical m/z value at 41.03913). Moreover, the ART-2a classification of HR-SPAMS data would generate more particle types compared to the classification results of LR-SPAMS data. All the codes for the automatic linear calibration method are open access and can be found at https://github.com/zhuxiaoqiang-fdu/zhuxiaoqiang-fdu.

Author Contribution

Y.X and X.W. supervised this study. X.W. and S.Z. designed the calibration and data analysis methods. S. Wang. and S.Z. performance the sea spray aerosol and ambient aerosol experiment. S.Z. wrote the open source code for calibration and data analysis of the single particle mass spectra and made the GUI program with suggestions from X.W. and X.Y.. X.W. and S.Z. prepared the manuscript with contributions from all co-authors.

Acknowledgments

This work was partially supported by the National Natural Science Foundation of China (Nos. 41827804, 41775150, 21906024, 91544224) and Shanghai Natural Science Foundation (No. 19ZR1404000). The authors thank Hexin Analytical Instrument Co., Ltd., China for providing HR-SPAMS.

Competing interests

The authors declare that they have no conflict of interest.

https://doi.org/10.5194/amt-2019-489
Preprint. Discussion started: 9 March 2020

Atmospheric Measurement Techniques Discussions

Reference

Ackerman, A. S., Kirkpatrick, M. P., Stevens, D. E., and Toon, O. B.: The impact of humidity above stratiform clouds on indirect aerosol climate forcing, Nature, 432, 1014-1017, 2004.

Bertram, T. H., Cochran, R. E., Grassian, V. H., and Stone, E. A.: Sea spray aerosol chemical composition: elemental and molecular mimics for laboratory studies of heterogeneous and multiphase reactions, Chemical Society Reviews, 2018. 10.1039.C1037CS00008A, 2018.

Chudinov, A., Li, L., Zhou, Z., Huang, Z., Gao, W., Yu, J., Nikiforov, S., Pikhtelev, A., Bukharina, A., and Kozlovskiy, V.: Improvement of peaks identification and dynamic range for bi-polar Single Particle Mass Spectrometer, International Journal of Mass Spectrometry, 436, 7-17, 2019.

Collins, D. B., Zhao, D. F., Ruppel, M. J., Laskina, O., Grandquist, J. R., Modini, R. L., Stokes, M. D., Russell, L. M., Bertram, T. H., and Grassian, V. H.: Direct aerosol chemical composition measurements to evaluate the physicochemical differences between controlled sea spray aerosol generation schemes, Atmospheric Measurement Techniques Discussions, 7, 6457-6499, 2014.

Li, L., Liu, L., Xu, L., Li, M., Li, X., Gao, W., Huang, Z., and Cheng, P.: Improvement in the Mass Resolution of Single Particle Mass Spectrometry Using Delayed Ion Extraction, Journal of the American Society for Mass Spectrometry, 29, 2105-2109, 2018.

Manuel, D. O., Harrison, R. M., Beddows, D. C. S., Freney, E. J., Heal, M. R., and Donovan, R. J.: Single-particle detection efficiencies of aerosol time-of-flight mass spectrometry during the North Atlantic marine boundary layer experiment, Environmental Science Technology, 40, 5029-5035, 2006.

Moffet, R. C. and Prather, K. A.: In-situ measurements of the mixing state and optical properties of soot with implications for radiative forcing estimates, Proceedings of the National Academy of Sciences of the United States of America, 106, 11872-11877, 2009.

Murphy, D. M.: The design of single particle laser mass spectrometers, Mass Spectrometry Reviews, 26, 150-165, 2010.

Nash, D. G., Baer, T., and Johnston, M. V.: Aerosol mass spectrometry: An introductory review, International Journal of Mass Spectrometry, 258, 2-12, 2006.

Pratt, K. A. and Prather, K. A.: Mass spectrometry of atmospheric aerosols-Recent developments and applications. Part II: On-line mass spectrometry techniques, Mass Spectrometry Reviews, 31, 17-48, 2012.

Qin, X., Bhave, P. V., and Prather, K. A.: Comparison of Two Methods for Obtaining Quantitative Mass Concentrations from Aerosol Time-of-Flight Mass Spectrometry Measurements, Analytical Chemistry, 78, 6169-6178, 2006.

Reinard, M. S., Adou, K., Martini, J. M., and Johnston, M. V.: Source characterization and identification by real-time single particle mass spectrometry, Atmospheric Environment, 41, 9397-9409, 2007.

Song, X.-H., Hopke, P. K., Fergenson, D. P., and Prather, K. A.: Classification of Single Particles Analyzed by ATOFMS Using an Artificial Neural Network, ART-2A, Analytical Chemistry, 71, 860-865, 1999.

Sullivan, R. C. and Prather, K. A.: Recent advances in our understanding of atmospheric chemistry and climate made possible by on-line aerosol analysis instrumentation, Analytical Chemistry, 77, 3861-3885, 2005.

https://doi.org/10.5194/amt-2019-489
Preprint. Discussion started: 9 March 2020

Atmospheric Measurement Techniques Discussions

372 Tsunogai, S., Saito, O., Yamada, K., and Nakaya, S.: Chemical composition of oceanic aerosol, Journal of
373 Geophysical Research, 77, 5283-5292, 1972.

374 Wang, H., An, J., Shen, L., Zhu, B., Xia, L., Duan, Q., and Zou, J.: Mixing state of ambient aerosols in Nanjing
375 city by single particle mass spectrometry, Atmospheric Environment, 132, 123-132, 2016.

376 Wang, H., Shen, L., Yin, Y., Chen, K., Chen, J., and Wang, Y.: Characteristics and mixing state of aerosol at
377 the summit of Mount Tai (1534 m) in Central East China: First measurements with SPAMS,
378 Atmospheric Environment, 213, 273-284, 2019.

379 Wenzel, R. J., Liu, D. Y., Edgerton, E. S., and Prather., K. A.: Aerosol time - of - flight mass spectrometry
380 during the Atlanta Supersite Experiment: 2. Scaling procedures, Journal of Geophysical Research:
381 Atmospheres, 2003. 2003.

382 Zelenyuk, A. and Imre, D.: Beyond single particle mass spectrometry: multidimensional
383 characterisation of individual aerosol particles, International Reviews in Physical Chemistry, 28, 309-
384 358, 2009.

385 Zhang, G., Bi, X., Chan, L. Y., Wang, X., Sheng, G., and Fu, J.: Size-segregated chemical characteristics of
386 aerosol during haze in an urban area of the Pearl River Delta region, China, Urban Climate, 4, 74-84,
387 2013.

388 Zhang, R. J. and Kin-Fai, H. O.: The Role of Aerosol in Climate Change,the Environment,and Human
389 Health, Atmospheric Oceanic Science Letters, 5, 156-161, 2012.
390

391

392

393

394

395

https://doi.org/10.5194/amt-2019-489
Preprint. Discussion started: 9 March 2020

Atmospheric Measurement Techniques Discussions

Figure Captions

Figure 1. The GUI program for HR-SPAMS calibration

Figure 2. Linear calibration with reference ion peaks

Figure 3. Probability distributions of the marker peak locations before and after Automatic Linear Calibration (AL-Cal) for (a) sea spray aerosol and (b) ambient aerosol

Figure 4. Averaged positive and negative mass spectra of sea spray aerosols

Figure 5. Averaged positive and negative mass spectra of ambient aerosols

Figure 6. Time series of peak intensities at m/z 40.95 and m/z 41.01

https://doi.org/10.5194/amt-2019-489
Preprint. Discussion started: 9 March 2020

Atmospheric Measurement Techniques Discussions

406 Table 1. Possible peak assignments for the m/z of reference ions for sea spray aerosol and
407 ambient aerosol

Unit mass resolution m/z	Possible species (Sea spray aerosol)	Unit mass resolution m/z	Possible species (Ambient aerosol)
+24	Mg^+ C_2^+	+39	K^+ $C_3H_3^+$
+39	K^+ $C_3H_3^+$	+56	Fe^+ Si_2^+ CaO^+ KOH^+
+81	Na_2Cl^+ Br^+ $C_6H_9^+$	-26	CN^- BO^- $C_2H_2^-$
+113	K_2Cl^+ $C_9H_5^+$	-62	NO_3^- $C_5H_2^-$
+115	K_2Cl^+ $C_9H_7^+$	-96	SO_4^- $BrOH^-$
-26	CN^- BO^- $C_2H_2^-$	-97	HSO_4^- C_8H^- BrO^- $NaCl_2^-$ $H_2PO_4^-$
-37	Cl^- C_3H^-		
-42	BO_2^- CNO^-		
-129	$MgCl_3^-$ $C_{10}H_9^-$ $(C_3H_7)_2C_2H_5^-$ $CaCl_2OH^-$		
-131	$MgCl_3^-$		

408
409
410
411
412
413
414

https://doi.org/10.5194/amt-2019-489
Preprint. Discussion started: 9 March 2020

Atmospheric Measurement Techniques Discussions

415 Table 2. Peak identification of important chemical species in sea spray aerosols. The first
416 column is the measured m/z for peaks. The second and third columns shows the theoretical
417 m/z bin value and theoretical m/z value of most possible specie for each peak

Measurement m/z(positive)	Possible species (theoretical m/z bin value)	Possible species (theoretical m/z value)	Measurement m/z(negative)	Possible species (theoretical m/z bin value)	Possible species (theoretical m/z value)
22.993	Na^+(22.993)	Na^+(22.98977)	15.0344	CH_3^-(15.0216)	CH_3^-(15.02348)
23.9829	Mg^+(23.9829)	Mg^+(23.98505)	34.9641	Cl^-(34.9641)	Cl^-(34.96885)
27.0267	$C_2H_3^+$(27.0267)	$C_2H_3^+$(27.02348)	41.9864	CNO^-(41.9971)	CNO^-(41.99799)
38.9672	K^+(38.9672)	K^+(38.96371)	25.0163	C_2H^-(25.0081)	C_2H^-(25.00783)
39.9711	Ca^+(39.9607)	Ca^+(39.96259)	38.0024	$C_3H_2^-$(38.0126)	$C_3H_2^-$(38.01565)
43.9614	CS^+(43.9723)	CS^+(43.9721)	44.9883	HCO_2^-(44.9994)	HCO_2^-(44.99767)
45.983	Na_2^+(45.983)	Na_2^+(45.97954)	49.002	C_4H^-(49.0135)	C_4H^-(49.00783)
59.9569	SiO_2^+(59.9696)	SiO_2^+(59.96677)	57.9574	$NaCl^-$(57.9574)	$NaCl^-$(57.95865)
71.9872	C_6^+(72.0012)	C_6^+(72)			
80.9438	Na_2Cl^+(80.9438)	Na_2Cl^+(80.94839)	63.9574	SO_2^-(63.9574)	SO_2^-(63.96191)
112.898	K_2Cl^+(112.898)	K_2Cl^+(112.89627)	75.9498	SiO_3^-(75.9642)	SiO_3^-(75.96196)
138.89	$Na_3Cl_2^+$(138.907)	$Na_3Cl_2^+$(138.90702)			
140.897	$Na_3Cl_2^+$(140.897)	$Na_3Cl_2^+$(140.90407)	79.9547	SO_3^-(79.9547)	SO_3^-(79.95683)
			80.9015	Br^-(80.9164)	Br^-(80.91629)
			85.9484	$NaPO_2^-$(85.9484)	$NaPO_2^-$(85.95337)
			99.9499	$CaCO_3^-$(99.9499)	$CaCO_3^-$ (99.94735)
			109.917	$CaCl_2^-$(109.9)	$CaCl_2^-$(109.9003)
			128.901	$MgCl_3^-$(128.883)	$MgCl_3^-$ (128.89161)

418
419
420
421
422
423
424

https://doi.org/10.5194/amt-2019-489
Preprint. Discussion started: 9 March 2020

Atmospheric Measurement Techniques Discussions

425 Table 3. Peak identification of important chemical species in ambient aerosols. The first
426 column is the measured m/z for each peak. The second and third columns shows the
427 theoretical m/z bin value and theoretical m/z value of most possible specie for each peak

Measurement m/z(positive)	Possible species(theoretical m/z bin value)	Possible species(theoretical m/z value)	Measurement m/z(negative)	Possible species(theoretical m/z bin value)	Possible species(theoretical m/z value)
22.993	Na^+(22.993)	Na^+(22.98977)	15.0408	CH_3^-(15.0216)	CH_3^-(15.02348)
23.9991	C_2^+(23.9991)	C_2^+(24)	16.0091	O^-(15.9959)	O^-(15.99492)
25.002	C_2H^+(25.0103)	C_2H^+(25.00783)	17.0145	OH^-(17.0009)	OH^-(17.00275)
26.0087	$C_2H_2^+$(26.0171)	$C_2H_2^+$(26.01565)	26.0078	CN^-(25.9994)	CN^-(26.00307)
30.0171	NO^+(29.999)	NO^+(29.99799)	31.987	O_2^-(31.987)	O_2^-(31.98984)
35.9925	C_3^+(36.0023)	C_3^+(36)	34.9641	Cl^-(34.9641)	Cl^-(34.96885)
36.9976	C_3H^+(37.0076)	C_3H^+(37.00783)	41.9971	CNO^-(41.9971)	CNO^-(41.99799)
38.0065	$C_3H_2^+$(38.0166)	$C_3H_2^+$(38.01565)	45.9897	NO_2^-(45.9897)	NO_2^-(45.99291)
38.9672	K^+(38.9672)	K^+(38.96371)	47.9911	C_4^-(47.993)	C_4^-(48)
47.993	C_4^+(47.993)	C_4^+(48)	61.9808	NO_3^-(61.9938)	NO_3^-(61.98783)
48.9911	C_4H^+(49.0026)	C_4H^+(49.00783)	71.0014	$C_3H_3O_2^-$(71.0153)	$C_3H_3O_2^-$(71.01332)
49.9994	$C_4H_2^+$(50.0111)	$C_4H_2^+$(50.01565)	78.9548	PO_3^-(78.9548)	PO_3^-(78.95852)
55.9443	Fe^+(55.932)	Fe^+(55.93494)	79.94	SO_3^-(79.9547)	SO_3^-(79.95683)
59.9951	C_5^+(59.9951)	C_5^+(60)	80.946	HSO_3^-(80.9609)	HSO_3^-(80.96466)
60.9946	C_5H^+(61.0074)	C_5H^+(61.00783)	95.9825	SO_4^-(95.9502)	SO_4^-(95.95175)
62.0023	$C_5H_2^+$(62.0152)	$C_5H_2^+$(62.01565)	96.9546	HSO_4^-(96.9546)	HSO_4^-(96.95958)
72.0012	C_6^+(72.0012)	C_6^+(72)	121.01	$C_{10}H^-$(121.01)	$C_{10}H^-$(121.00783)
84.0108	C_7^+(83.9957)	C_7^+(84)	122.01	$C_{10}H_2^-$(122.01)	$C_{10}H_2^-$(122.01565)
207.976	Pb^+(207.967)	Pb^+(207.97664)	134.008	$C_{11}H_2^-$(134.008)	$C_{11}H_2^-$(134.01565)

428
429
430

https://doi.org/10.5194/amt-2019-489
Preprint. Discussion started: 9 March 2020

Atmospheric Measurement Techniques Discussions

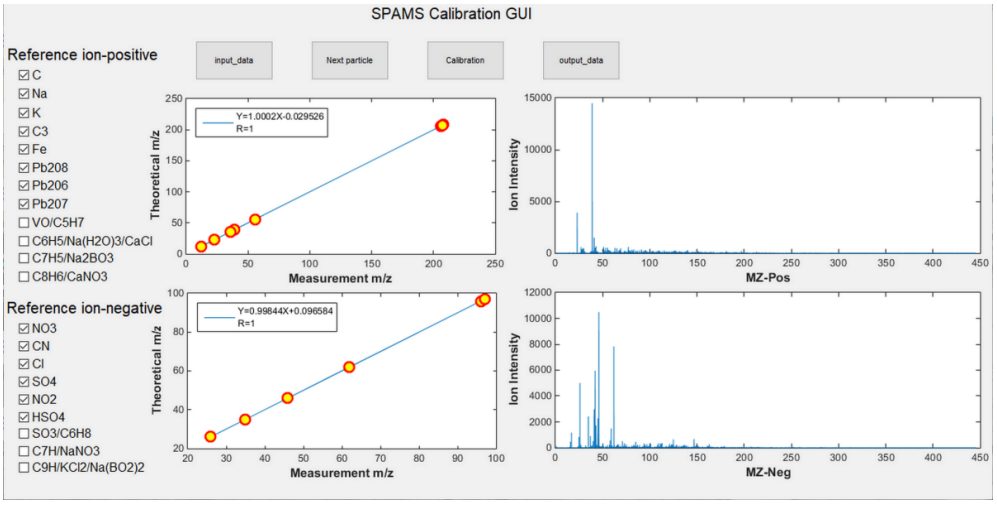

Figure 1. The GUI program for HR-SPAMS calibration

https://doi.org/10.5194/amt-2019-489
Preprint. Discussion started: 9 March 2020

Atmospheric Measurement Techniques Discussions

435

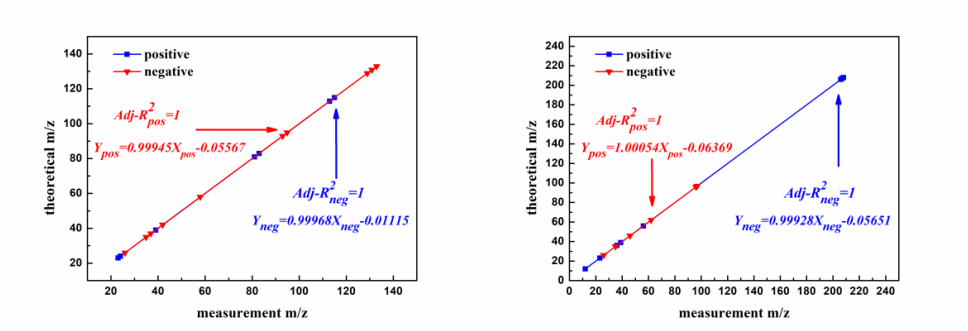

436

437 (a)sea spray aerosol (b)ambient aerosol

438

439 Figure 2. Linear calibration with reference ion peaks

440

441

442

443

444

445

446

447

448

449

450

451

452

https://doi.org/10.5194/amt-2019-489
Preprint. Discussion started: 9 March 2020

Atmospheric Measurement Techniques Discussions

453 a.

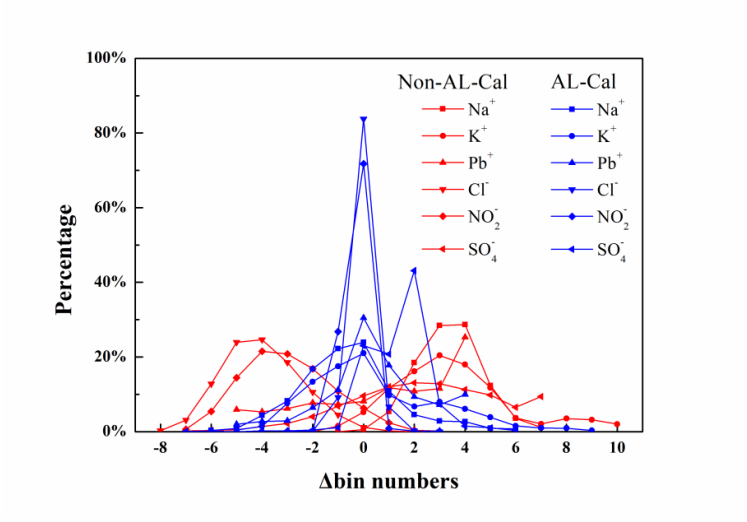

454

455 b.

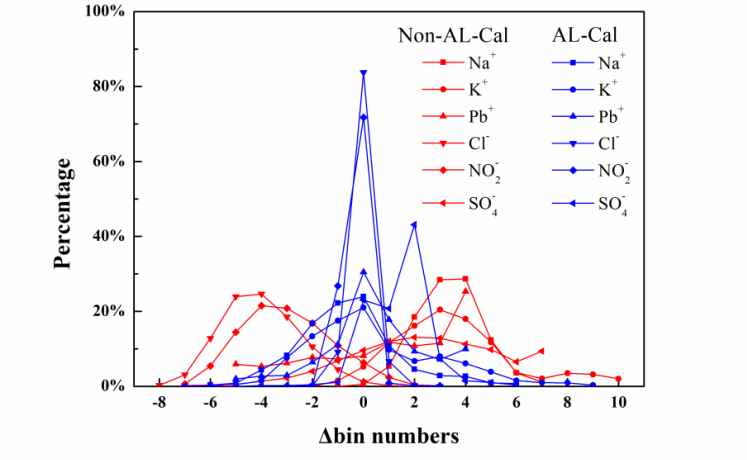

456

457 Figure 3. Probability distributions of the marker peak locations before and after Automatic
458 Linear Calibration (AL-Cal) for (a) sea spray aerosol and (b) ambient aerosol

459

https://doi.org/10.5194/amt-2019-489
Preprint. Discussion started: 9 March 2020

Atmospheric Measurement Techniques Discussions

460

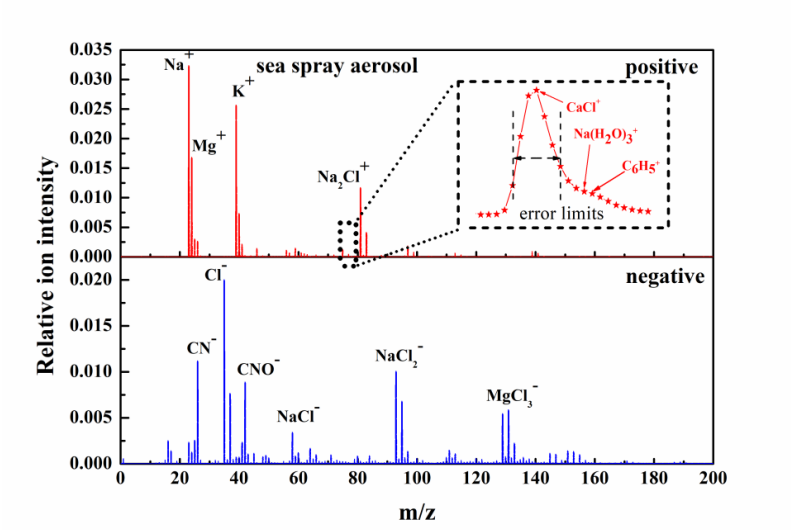

461

462 Figure 4. Averaged positive and negative mass spectra of sea spray aerosols

463

https://doi.org/10.5194/amt-2019-489
Preprint. Discussion started: 9 March 2020

Atmospheric Measurement Techniques Discussions

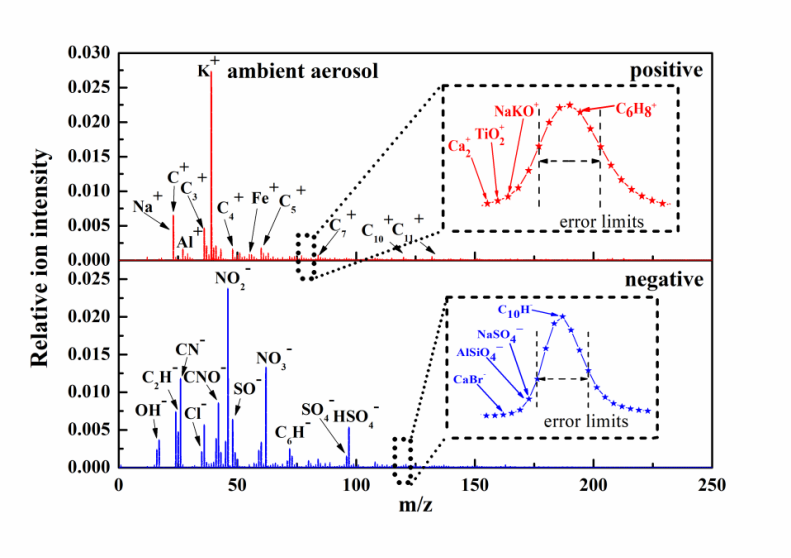

Figure 5. Averaged positive and negative mass spectra of ambient aerosols

https://doi.org/10.5194/amt-2019-489
Preprint. Discussion started: 9 March 2020

Atmospheric Measurement Techniques Discussions

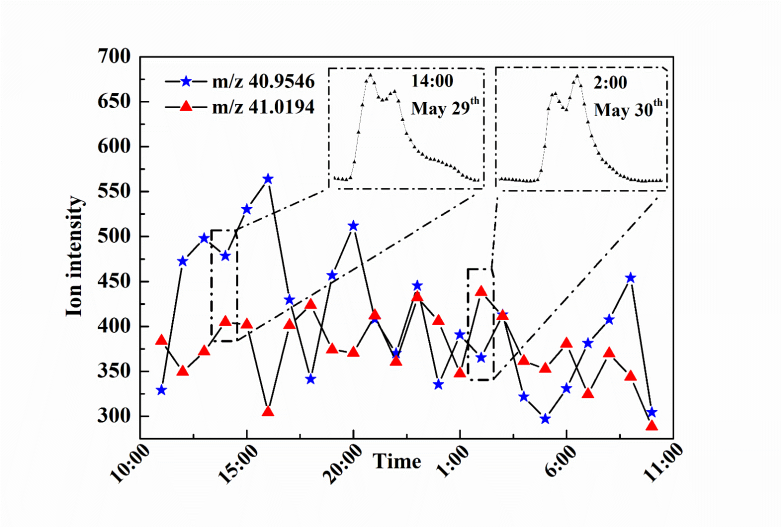

Figure 6. Time series of peak intensities at m/z 40.95 and m/z 41.01